

# Thermal Conductivity and Density of Plant Oils under High Pressure

Matthias Werner,<sup>†</sup> Albert Baars,<sup>‡</sup> Cornelia Eder,<sup>†</sup> and Antonio Delgado<sup>\*,§</sup>

Lehrstuhl für Systemverfahrenstechnik, Technische Universität München, D-85350 Freising, Germany, Hochschule Bremen, D-28199 Bremen, Germany, and Lehrstuhl für Strömungsmechanik, Friedrich-Alexander-Universität Erlangen-Nürnberg, D-91058 Erlangen, Germany

The effect of pressure on the thermal conductivity and density of olive, safflower, linseed, and castor oils in the temperature range of (283 to 333) K and pressures up to 400 MPa was studied. The thermal conductivity measurements were carried out using a transient hot-wire method with an estimated uncertainty of  $2.7 \text{ mW}\cdot\text{m}^{-1}\cdot\text{K}^{-1}$ . The density of olive oil was determined within an uncertainty of 0.3 % by a Jamin interferometer. Results reveal an increase in the thermal conductivity and density with pressure. The pressure dependency of the thermal conductivity of these plant oils correlates with the coefficient of isothermal compressibility. The temperature dependency of the thermal conductivity is linked to the isobaric thermal expansion coefficient. This agrees well with the vibrational theory of thermal conductivity due to Horrocks and McLaughlin. From this model, the relation between thermal conductivity and density  $\lambda/\lambda_0 = (\rho/\rho_0)^g$  can be obtained. The application of our data to this relation leads to  $g \approx 3$ , which is typical for organic liquids.

## Introduction

The use of hydrostatic pressures up to 1 GPa in bio- and food technology offers a variety of new possibilities. Pressure-induced modifications of inter- and intramolecular interactions permit the creation of new functionalities and structures of biomaterials.<sup>1</sup> Macroscopic properties such as viscosity,<sup>2</sup> thermal conductivity, diffusion coefficient, and therefore mass and energy transport during high-pressure treatment can thus be affected. Moreover, high-pressure treatment of foods facilitates a conservation at moderate temperatures. In contrast to conventional thermal conservation processes, essential food ingredients like vitamins and flavors are better preserved. However, the levels of harmful microorganisms and enzymes can be decreased to an acceptable magnitude,<sup>3,4</sup> too.

Pressure perturbances spread out at the speed of sound, which is much faster than energy transport by diffusion or convection in thermal processes. Thus, high-pressure treatment should lead to a more homogeneous chemical and biochemical conversion in comparison to thermal processes. Consequently, an improved product quality should be obtained, as biochemical reaction kinetics depend on pressure and temperature.<sup>5</sup>

However, numerous investigations<sup>6–9</sup> prove that inhomogeneous temperature fields occur in high-pressure chambers during the (de)compression phase and holding time. In a typical high-pressure process, the system consists of product, packaging, pressure transmitting fluid, and pressure vessel. The spatial distribution of these materials and their different physical properties leads to unequal, pressure-induced temperature

changes. As a result, diffusive and convective thermal transport processes appear in the chamber.

The knowledge about thermal physical properties of the involved media as a function of temperature and pressure is indispensable for comprehension and estimation of thermofluid dynamics during high-pressure processes. Besides density,<sup>10</sup> viscosity,<sup>11</sup> and thermal capacity, the thermal conductivity  $\lambda$  proves to be of great importance. The latter property describes the ability of a solid, liquid, or gas to transport thermal energy by means of molecular motion.

Pressure-dependent data of thermal conductivity regarding food and food ingredients are rare in the literature. Bridgman,<sup>12</sup> Lawson et al.,<sup>13</sup> and Kestin et al.<sup>14</sup> have published data for pure water. Abdulagatov and Magomedov<sup>15</sup> investigated food-relevant aqueous salt solutions (NaCl and KCl) in a large temperature range and at pressures up to 100 MPa. Denys and Hendrickx<sup>16</sup> published data of thermal conductivities for apple pulp and tomato paste up to 400 MPa. Ramaswamy et al.<sup>17</sup> provide data for canola oil, clarified butter, honey, high fructose corn syrup, and apple juice at 25 °C up to 700 MPa.

Nonpolar components such as plant oils are important in food technology. In this article, the effect of pressures up to 400 MPa on the thermal conductivity of different plant oils is investigated experimentally using a high-pressure-adapted transient hot-wire method.

Data of fats and oils are rare at ambient pressure. Table 1 gives an overview. Kaye and Higgins<sup>18</sup> published comprehensive thermal conductivity data for olive as well as castor oil in a large temperature range measured with a guarded parallel plate apparatus and a mentioned uncertainty of about  $\pm 1\%$ . Nowrey and Woodams<sup>19</sup> investigated the thermal conductivity of peanut and olive oil determined by a parallel plate method with an estimated uncertainty of  $\pm 2\%$ . Nesvadba<sup>20</sup> gives an average value of  $\lambda$  for olive oil from five laboratories, measured within the COST93 project. Qashou et al.,<sup>21</sup> Coupland and McClements,<sup>22</sup> Choi and Okos,<sup>23</sup> and Hemminger<sup>24</sup> provide further data for different oils.

\* To whom correspondence should be addressed. E-mail: antonio.delgado@lstm.uni-erlangen.de. Phone: ++49-(0)9131-85-29500. Fax: ++49-(0)9131-85-29503.

<sup>†</sup> Technische Universität München.

<sup>‡</sup> Hochschule Bremen.

<sup>§</sup> Friedrich-Alexander-Universität Erlangen-Nürnberg.

**Table 1. Thermal Conductivity Data of Some Plant Oils at Ambient Pressure**

oil	$T$	$\lambda$	$(d\lambda/dT)$	ref
	K	$\text{W}\cdot\text{m}^{-1}\cdot\text{K}^{-1}$	$10^{-4}\text{W}\cdot\text{m}^{-1}\cdot\text{K}^{-2}$	
Olive	273.2 to 473.2	0.1696 to 0.1574	-0.61	18
Olive	311.7	0.1679		19
	324.5	0.1627		
Olive	296.13	0.164		20
Castor	273.2 to 433.2	0.183 to 0.1683	-0.91	18
Canola	293.15	0.16		23
Canola	298.15	0.22 to 0.23		17
Linseed	303.15	0.17	-2.1	24
Almond	283.15	0.17		24
Peanut	297.5	0.1679		19
Poppy seed	283.15	0.16		24
Sesame	283.15	0.16		24
Butter oil	293.15	0.17		24

The comparison of the different plant oils in Table 1 shows that the thermal conductivity values lie in a small span between about  $(0.16 \text{ and } 0.18) \text{ W}\cdot\text{m}^{-1}\cdot\text{K}^{-1}$  with a very small negative temperature derivative  $d\lambda/dT$ . The measured values for canola oil from Ramaswamy et al.<sup>17</sup> seem to be unusually high compared to these of Choi and Okos<sup>23</sup> and the other data. Factors like climate, geography, plant variety, processing, purity, storage conditions, etc. influence the composition of the plant oils and thus its chemical and physical properties.<sup>22</sup> Deviations between the different data sets can therefore arise due to the naturally varying sample compositions in addition to the measuring uncertainties. Unfortunately, the compositions of the oils investigated in the literature were not given.

Previous investigations<sup>25–29</sup> on thermal conductivity  $\lambda$  of different pressurized liquids like alcohols, hydrocarbons, aqueous sugar solutions, etc. reveal a strong specific volume sensitivity. Thus, additional density measurements of olive oil were carried out in the temperature range from (293 to 333) K and pressures up to 400 MPa by high-pressure interferometry.<sup>10</sup> Acosta et al.<sup>30</sup> deliver further density data of plant oils up to pressures of about 150 MPa.

On the basis of the existing thermal conductivity and density data, thermal conductivity models for liquids under high pressure due to the vibrational theory of Horrocks and McLaughlin<sup>25–27,36,37</sup> were applied to plant oils in this work.

## Materials and Methods

**Materials.** In this work, the pressure effect up to 400 MPa on the thermal conductivity and density of four plant oils in the temperature range of (283 to 333) K was studied. The commercially available oils investigated, olive oil, safflower oil, linseed oil, and castor oil, are fatty-acid esters of glycerin (triglycerides) which differ in the concentration of unsaturated fatty acids:  $\text{C}_{18:1}$  (oleic),  $\text{C}_{18:2}$  (linoleic),  $\text{C}_{18:3}$  (linolenic), and  $\text{C}_{18:1}\text{-OH}$  (ricinoleic). The single fatty acid concentrations of the olive, safflower, and linseed oil were analyzed using a gas chromatography method (VDLUF A, III, 5.6.2/DGF C–VI 11e, Nutrition and Food Research Center, ZIEL, Technische Universität München, Germany) (Table 2). The results of the castor oil agree with the manufacturer's batch analysis certificate (method: PHEUR 5.0). The density  $\rho$  of the plant oils at ambient pressure and 293.2 K was measured by the oscillating U-tube method (uncertainty:  $\pm 0.1 \text{ kg}\cdot\text{m}^{-3}$ ). The density data at the other temperatures were determined by the temperature derivatives  $d\rho/dT$  given by Acosta et al.<sup>30</sup>

**High-Pressure Heat Conductivity Measurement Technique.** For the experimental investigation of the thermal conductivity  $\lambda$  of liquids under pressure, different systems have

been described in the literature. Bridgman<sup>12</sup> and Lawson et al.<sup>13</sup> used a steady-state coaxial-cylinder method for low viscous liquids up to pressures of 1200 MPa. Denys and Hendrickx<sup>16</sup> as well as Ramaswamy et al.<sup>17</sup> studied different liquid foods up to 700 MPa using a line-heat source probe method. The first systems are rather complex in construction. The applicability to low viscous liquids of the second system is naturally limited due to the thermal inertia of the thermocouple probes. A calibration is additionally necessary, based on a water–agar gel system<sup>16</sup> or pure water.<sup>17</sup> Nieto de Castro et al.<sup>31</sup> used a transient hot-wire method for thermal conductivity investigations of toluene in the temperature range  $T = (308 \text{ to } 363) \text{ K}$  and pressures as high as 600 MPa. This measurement device works with a differential hot-wire principle together with a special measuring bridge. The uncertainty is about 1 %.

In this contribution, a high-pressure modification<sup>29</sup> of the classical transient hot-wire method<sup>32</sup> was used. This allows short measurement periods to be realized to reduce the influence of free convection and enables investigations of low viscosity liquids. A  $25 \mu\text{m}$  thin platinum wire acts both as a fast heating source and as a temperature sensor. Initially, the wire and the surrounding liquid are characterized by a uniform temperature field. During the measurement, the wire is heated by a constant current (DC) for a few seconds. This results in a temporal temperature increase of the wire and the surrounding liquid. This depends mainly on the thermal conductivity of the liquid sample. Details about the thermal conductivity determination and sensor calibration are described elsewhere.<sup>29</sup>

The hot-wire sensor is embedded in an autoclave with a maximum working pressure of 450 MPa, 28 mm inner diameter, 170 mm usable inner height, and with a volume of  $100 \text{ cm}^3$ . Details of the measurement setup are provided as Supporting Information (Figure S1). The pressure is generated by a motor-driven spindle pump (type 750.1700, Sieber Sitec Engineering Corp., Switzerland) and monitored by a pressure gauge (type EBM 6045.V/4–20/7000, Brosa Corp., Germany) with an uncertainty of  $\pm 1.75 \text{ MPa}$  (related to the displayed value). The investigated fluid is also the pressure-transmitting medium. The small pump volume ( $4 \text{ cm}^3$ ) affords an additional valve for reloads between the pump and autoclave. A thermostat pump unit (P1C45P, Thermo Corp., Germany) together with a thermo-jacket permit temperature settings in the range from (253 to 363) K. The temperature in the vessel is detected by a digital thermometer (GMH3050, Greisinger Corp., Germany) with a thermocouple sensor (type T class 1, TC Mess- and Regeltechnik Corp., Germany) and a resolution of  $\pm 0.1 \text{ K}$ . After a few pressure treatments of the thermocouple tip, the thermocouple in the vessel was calibrated at ambient pressure using a high-precision thermometer (P550, Dostmann Electronic Corp., Germany) with a resolution of  $\pm 0.03 \text{ K}$ . The temperature measurement uncertainty was  $\pm 0.13 \text{ K}$ . It is assumed that the pressure effect on the temperature sensor was negligibly small.

The electronic part consists of a computer-controlled measuring bridge described by Greger<sup>32</sup> with some modifications. The reference voltage  $U_{\text{ref}}$  for the zero adjustment of the instrumental amplifier (AD624, Analog Devices, USA) was delivered from the analog outputs  $[(-10 \text{ to } 10) \text{ V}]$  of a 16-bit A/D-D/A converter PC card (PCI-MIO-XE10, National Instruments, Germany) before measurement started. The large spans of software-adjustable reference voltage and heating current enable measurements in a wide thermal conductivity range without any changes to the bridge circuit hardware. The voltage drop over the hot-wire during measurement was compared with the reference value,  $U_{\text{ref}}$ . The difference was amplified by a factor

**Table 2. Physico-Chemical Properties of the Investigated Plant Oils at 293.2 K**

oil	$\rho$ kg·m <sup>-3</sup>	$d\rho/dT^{30}$ 10 <sup>-3</sup> kg·m <sup>-3</sup> ·K <sup>-1</sup>	fatty acid concentration (g per 100 g of total fatty acids)						
			C <sub>16</sub>	C <sub>16:1</sub>	C <sub>18</sub>	C <sub>18:1</sub>	C <sub>18:2</sub>	C <sub>18:3</sub>	other
Olive <sup>a</sup>	912.7	-554.1	11.6	0.8	3.7	75.3	6.7	0.7	0.1
Safflower <sup>b</sup>	922.8	-629.7	5.6	0.1	2.3	10.9	79.1	0.2	0.0
Linseed <sup>c</sup>	927.7	-641.9	5.0	0.0	3.5	16.3	15.2	58.7	0.0
Castor <sup>d</sup>	959.2	-648.4	1.2	0.0	1.1	3.3	5.7	0.6	87.6 (ricinoleic)

<sup>a</sup> Cantinelle, native extra, Aldi Corp. Germany, BBD\* 02.10.06 (CAS Registry No.: 8001-25-0). <sup>b</sup> Bellasan, Brökelmann & Co Oelmühle Corp., Germany, BBD 20.09.07 (CAS Registry No.: 8001-23-8). <sup>c</sup> Food linseed oil, Schneekoppe Corp., Germany, BBD 28.08.06 (CAS Registry No.: 8001-26-1). <sup>d</sup> Caelo, native, W429 (PZN 0466804), Caesar & Lorentz Corp., Germany, BBD 03/2007 (CAS Registry No.: 8001-79-4). \*BBD: Best Before Date.

of 500 and converted digitally by the PC card in the DAQ computer. The thermometer, pressure indicator, and thermostat pump were connected to the RS 232 serial-interface ports for signal recording. As measurement and visualization software, LabView (National Instruments) was used.

The hot-wire sensor (Figure 1) was directly connected at the high-pressure lid seal plug and linked to the bridge circuit via high-pressure electrical feedthrough (Sitec) and shielded cable (four-point connection). The ends of the thin platinum wire (diameter 25  $\mu$ m, length 110 mm) were soldered into small brass pins. The upper one was fixed in an isolated plate. The lower one was connected to a weight to keep the wire linear in the vertical direction. The pressure was assumed to have an insignificant effect on wire diameter and length. The two electrical contacts for the voltage metering during the experimental process were spot-welded at a distance from the soldering points of the hot-wire to reduce fringe effects.

The standard uncertainty of the measurement system is about 2.7 mW·m<sup>-1</sup>·K<sup>-1</sup> and was derived on the basis of error propagation calculations, including all uncertainties of the involved system components.

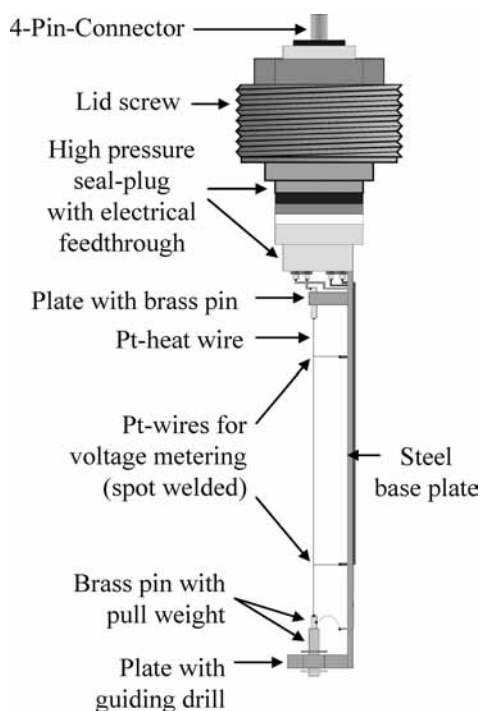
**Experimental Procedure.** First, the investigated oils were heated up to about 333 K to melt all existing fat crystals. The samples were then degassed for about 10 min using the vacuum from a water-jet pump. After the system was filled with a squeeze pump and a high-pressure spindle pump, the pressure

was stabilized manually via a motor control unit to  $\pm 0.1$  MPa. Once thermal equilibrium of the fluid in the pressurized autoclave was reached, the thermal conductivity measurement started.

Due to the increase of the crystallization temperature of plant oils with rising pressure,<sup>33</sup> the maximum working pressure had to be reduced with decreasing measurement temperatures. This was necessary to avoid a mechanical destruction of the sensitive Pt hot-wire due to the formation of crystal structures in the sample. Temperature and thermal conductivity data are averaged values from three to six measurements.

**High-Pressure Density Measurement Technique.** The pressure effect on the density of olive oil was measured utilizing a high-pressure Jamin interferometer. Details of this device are described elsewhere.<sup>10</sup> The estimated uncertainty is  $\pm 0.3$  %.

For the high-pressure density data of the other three oils,  $pVT$  data from the literature were used. Acosta et al.<sup>30</sup> determined the density of olive, safflower, linseed, and castor oils. The measurements were carried out using a static-type bellows apparatus (uncertainty 0.1 %) at pressures of up to 144 MPa in the temperature range from (303 to 353) K. Besides experimental data of specific volumes, parameters of the Tait equation were given. The unavailable density data  $\rho(p,T)$  for the pressure range above 144 MPa were estimated by extrapolation using the Tait equation. The estimation of the uncertainty of the extrapolated values was reviewed through comparison with our experimental data of  $\rho(p,T)$  for olive oil.

**Figure 1.** High-pressure hot-wire probe.

## Results

**Thermal Conductivity Measurements in Toluene.** To verify the accuracy of the system, a comparison of our measurements with literature data for toluene was carried out. For this, pressures up to 400 MPa in the temperature range from (273 to 330) K were applied. The purity of the toluene (VWR, No. 1.108323.1000) was 99.9 %. The present results show a maximum standard deviation of 0.3 mW·m<sup>-1</sup>·K<sup>-1</sup> and agree well with data from the literature<sup>31,34,35</sup> (see Figure 2). Nevertheless, there seems to be a growing deviation with increasing pressure. The deviations are within the uncertainty of the measurement system. Therefore, this has not been investigated further. The uncertainty of the IUPAC (International Union of Pure and Applied Chemistry) and high-pressure thermal conductivity data for toluene of Nieto de Castro et al.<sup>31,35</sup> was estimated as  $\pm 1.0$  % and that of Ramires et al.<sup>34</sup> as  $\pm 0.5$  %.

**Thermal Conductivity of Plant Oils.** Tables 3 to 6 contain the arithmetic means of the experimental thermal conductivity results for the different oils and the corresponding standard deviations. For equal temperatures at ambient pressure, the values of olive, safflower, and linseed oil are around 7 % lower in comparison to those of castor oil. Reasons for these

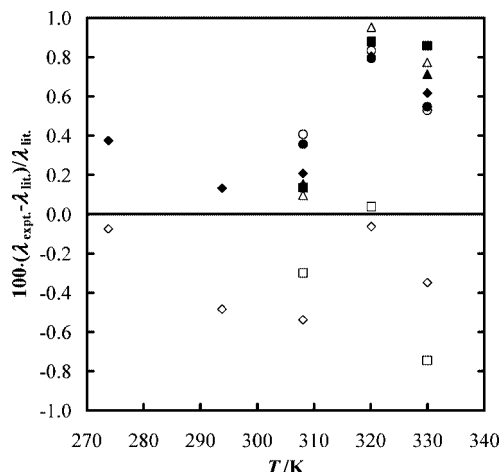


**Figure 2.** Relative deviations between experimental results and literature data of thermal conductivity  $\lambda$  for toluene at different temperatures and pressures:  $\diamond$ , 0.1 MPa;<sup>34</sup>  $\blacklozenge$ , 0.1 MPa;<sup>35</sup>  $\square$ , 0.1 MPa;  $\triangle$ , 50 MPa;  $\blacksquare$ , 100 MPa;  $\blacktriangle$ , 200 MPa;  $\circ$ , 300 MPa;  $\bullet$ , 400 MPa.<sup>31</sup>

differences are likely to be found in the different molecular structure of the oils. This will be discussed later.

The deviations between our results for olive and castor oil in relation to published data (Table 1) at ambient pressure are in the range of (+1.2 to -2) %. Apart from newer data of olive oil from Nesvadba<sup>20</sup> at  $T = 296$  K, nearly all other values show negative deviations.

To visualize the influence of  $p$  and  $T$ , the normalized relative thermal conductivity  $\lambda_r(p) = \lambda(p)/\lambda(p_0)$  was plotted versus normalized pressure  $p_r = p/p_0$ , whereas  $p_0$  represents the ambient pressure. This is shown for olive oil in Figure 3. The general tendency reflects an increase of  $\lambda_r$  with increasing pressure and temperature. The slopes of the isotherms reduce with rising  $p_r$ . By plotting  $\lambda$  versus  $T$  (Figure 4), an almost linear relationship of the isobars with increasing pressure can be observed. Furthermore, the initial negative value of the temperature derivative  $d\lambda/dT$  at ambient pressure changes its sign at a pressure of about 100 MPa. This behavior arises qualitatively for the other three oils, too. Nevertheless, the slope of  $\lambda_r$  versus  $p_r$  differs with growing  $p_r$  (see Figure 5 for 333 K). The highest increase can be observed for olive oil, followed by safflower, linseed, and castor oil.

The value of  $\lambda_r \approx 1.18$  published for canola oil<sup>17</sup> at  $p_r = 2000$  and  $T = 298.15$  K is considerably lower compared to those reported here ( $\lambda_r \approx 1.24$  to 1.27). Moreover, the linear relation between  $\lambda$  and  $p$  given by Ramaswamy et al.<sup>17</sup> can not be confirmed.

**High-Pressure Density of Plant Oils.** Our experimental results of the relative density  $\rho_r(p) = \rho(p)/\rho(p_0)$  for olive oil at pressures up to 434 MPa in the temperature range from (293 to 333) K are provided in Table 7. Figure 6 displays  $\rho_r$  as a function of  $p_r$  at five different temperatures. At constant pressure,  $\rho_r$  increases with increasing temperature, and the slopes of the isotherms reduce with rising  $p_r$ .

The comparison between data from Acosta et al.<sup>30</sup> for the density of olive oil (extrapolated up to 400 MPa via the Tait equation) and measured values shows deviations in the range from (-0.34 to +0.32) %. On the basis of these results, the density data of safflower, linseed, and castor oil up to 400 MPa were calculated via the Tait equation according to data from Acosta et al.<sup>30</sup> Figure 7 illustrates the normalized density data for all four investigated oils at 333 K and relative pressures  $p_r$  up to 4000. For all chosen temperatures, the highest increase

of  $\rho_r$  with  $p_r$  can be observed for olive oil and the lowest for castor oil. From the similar behavior of  $\lambda_r(p, T)$  and  $\rho_r(p, T)$ , one can conclude that a correlation between the transport property and the state variable exists. This will be discussed in the following section.

## Discussion

The results of thermal conductivity and density demonstrate a qualitatively similar behavior regarding pressure and temperature but also among the different oils. According to this,  $\rho_r$  and thus  $\lambda_r$  seem to decrease from olive oil via safflower oil to linseed oil and castor oil. Reasons for this behavior are likely to be found in the molecular structure of the oils. This will be discussed at the end of this section.

The literature designates different theories concerning the thermal conductivity  $\lambda$  of liquids. In the following, some of these theories<sup>25–27</sup> which especially consider the temperature and density dependency of  $\lambda$  under high pressures were applied to our experimental data. The determination of the transport property by molecular dynamic simulation was not examined in this study.

Horrocks and McLaughlin<sup>36,37</sup> as well as Kamal and McLaughlin<sup>25</sup> deduced a relation for the thermal conductivity of liquids on the basis of the vibrational theory:<sup>36</sup>

$$\lambda = \sqrt{2} \nu c_v a^{-1} \quad (1)$$

Here,  $a$  represents the shortest distance between adjacent molecules in a quasilattice structure,  $\nu$  their mean vibrational frequency, and  $c_v$  the heat capacity per molecule which is associated with the transport process. In this model, one presumes that the molecules are located in a quasilattice (face-centered cube arrangement) vibrating inharmoniously at their equilibrium position. The net thermal energy transport occurs through collisions between molecules in the direction of the negative temperature gradient. The contribution due to Brownian motion has been shown to be small<sup>36</sup> and is therefore not considered in eq 6.

McLaughlin and colleagues<sup>27</sup> assumed  $c_v$  to be independent of  $T$  and  $\rho$ , and together with  $a^{-1} \sim (\rho_r)^{1/3}$  and eq 1 one obtains

$$\lambda \sim \nu(\rho_r)^{1/3} \quad (2)$$

Using this approach in combination with the thermodynamic expressions<sup>27</sup>

$$\frac{1}{\lambda} \left( \frac{\partial \lambda}{\partial p} \right)_T = \kappa_T \frac{\rho}{\lambda} \left( \frac{\partial \lambda}{\partial \rho} \right)_T \quad (3)$$

and

$$\frac{1}{\lambda} \left( \frac{\partial \lambda}{\partial T} \right)_p = \frac{1}{\lambda} \left( \frac{\partial \lambda}{\partial T} \right)_\rho - \alpha_p \frac{\rho}{\lambda} \left( \frac{\partial \lambda}{\partial \rho} \right)_T \quad (4)$$

they finally derived eq 5 and eq 6 for the temperature and pressure coefficients of thermal conductivity,  $(1/\lambda)(\partial\lambda/\partial T)_p$  and  $(1/\lambda)(\partial\lambda/\partial p)_T$ .

$$\frac{1}{\lambda} \left( \frac{\partial \lambda}{\partial T} \right)_p = \frac{1}{\nu} \left( \frac{\partial \nu}{\partial T} \right)_\rho - \alpha_p \left( \frac{1}{3} + \gamma_G \right) \quad (5)$$

$$\frac{1}{\lambda} \left( \frac{\partial \lambda}{\partial p} \right)_T = \kappa_T \left( \frac{1}{3} + \gamma_G \right) \quad (6)$$

Here,  $\alpha_p$  represents the isobaric coefficient of thermal expansion and  $\kappa_T$  the isothermal compressibility. The Grüneisen  $\gamma_G$  parameter

**Table 3.**  $p\lambda T$  Data for Olive Oil with Standard Deviations in Brackets

$p$	$T$	$\lambda$	$T$	$\lambda$	$T$	$\lambda$	$T$	$\lambda$
MPa	K	$\text{mW}\cdot\text{m}^{-1}\cdot\text{K}^{-1}$	K	$\text{mW}\cdot\text{m}^{-1}\cdot\text{K}^{-1}$	K	$\text{mW}\cdot\text{m}^{-1}\cdot\text{K}^{-1}$	K	$\text{mW}\cdot\text{m}^{-1}\cdot\text{K}^{-1}$
0.1	283.1	167.2 (0.1)	293.7	166.1 (0.1)	314.2	164.4 (0.1)	334.6	162.8 (0.3)
25	283.2	174.1 (0.1)	293.5	173.5 (0.2)	314.1	172.1 (0.1)	334.4	170.6 (0.6)
50	283.2	180.2 (0.1)	293.5	179.1 (0.1)	314.0	178.5 (0.1)	334.6	178.0 (0.1)
100	283.2	189.2 (0.2)	293.4	190.0 (0.1)	313.9	189.8 (0.1)	334.5	190.2 (0.1)
150			293.4	199.8 (0.2)	313.9	200.3 (0.1)	334.4	200.6 (0.2)
200			293.5	208.5 (0.2)	313.9	209.4 (0.1)	334.5	210.3 (0.1)
250					313.8	217.8 (0.2)	334.5	220.3 (0.1)
300					313.9	225.7 (0.1)	334.3	227.2 (0.2)
350							334.3	234.8 (0.1)
400							334.4	242.0 (0.3)

**Table 4.**  $p\lambda T$  Data for Safflower Oil with Standard Deviations in Brackets

$p$	$T$	$\lambda$	$T$	$\lambda$	$T$	$\lambda$	$T$	$\lambda$
MPa	K	$\text{mW}\cdot\text{m}^{-1}\cdot\text{K}^{-1}$	K	$\text{mW}\cdot\text{m}^{-1}\cdot\text{K}^{-1}$	K	$\text{mW}\cdot\text{m}^{-1}\cdot\text{K}^{-1}$	K	$\text{mW}\cdot\text{m}^{-1}\cdot\text{K}^{-1}$
0.1	283.1	165.4 (0.1)	293.2	164.8 (0.1)	313.3	163.5 (0.1)	333.2	161.6 (0.1)
25	283.2	171.9 (0.1)	293.2	171.5 (0.1)	313.3	170.9 (0.1)	333.0	170.2 (0.1)
50	283.2	177.3 (0.1)	293.2	177.3 (0.2)	313.1	177.1 (0.1)	333.2	176.7 (0.0)
100	283.1	187.4 (0.1)	293.0	187.5 (0.1)	313.1	188.0 (0.2)	333.1	188.7 (0.2)
150			293.2	196.5 (0.1)	313.2	197.2 (0.1)	333.2	198.4 (0.3)
200			293.0	204.6 (0.1)	313.2	205.8 (0.1)	333.2	206.6 (0.1)
250					313.2	213.5 (0.1)	333.1	215.7 (0.2)
300					313.2	220.8 (0.1)	333.1	223.5 (0.1)
350							333.1	230.7 (0.1)
400							333.1	237.4 (0.1)

**Table 5.**  $p\lambda T$  Data for Linseed Oil with Standard Deviations in Brackets

$p$	$T$	$\lambda$	$T$	$\lambda$	$T$	$\lambda$	$T$	$\lambda$
MPa	K	$\text{mW}\cdot\text{m}^{-1}\cdot\text{K}^{-1}$	K	$\text{mW}\cdot\text{m}^{-1}\cdot\text{K}^{-1}$	K	$\text{mW}\cdot\text{m}^{-1}\cdot\text{K}^{-1}$	K	$\text{mW}\cdot\text{m}^{-1}\cdot\text{K}^{-1}$
0.1	282.6	165.7 (0.1)	292.7	165.2 (0.3)	313.3	164.0 (0.2)	333.4	162.4 (0.2)
25	282.6	172.0 (0.1)	292.8	171.6 (0.2)	313.3	170.6 (0.4)	333.3	170.0 (0.1)
50	282.5	177.7 (0.1)	292.7	177.2 (0.1)	313.2	176.6 (0.3)	333.3	176.7 (0.1)
100	282.5	187.6 (0.2)	292.7	187.5 (0.1)	313.2	187.6 (0.3)	333.3	188.4 (0.1)
150			292.6	196.4 (0.1)	313.1	196.9 (0.2)	333.3	198.6 (0.2)
200			292.6	204.5 (0.1)	313.1	205.4 (0.3)	333.3	207.5 (0.2)
250					313.0	213.4 (0.1)	333.3	215.7 (0.1)
300					313.0	220.8 (0.1)	333.3	223.2 (0.1)
350							333.3	230.2 (0.1)
400							333.3	236.9 (0.3)

$$\gamma_G = \frac{\rho}{\nu} \left( \frac{\partial \nu}{\partial \rho} \right)_T \quad (7)$$

characterizes the relationship between mean molecular vibration frequency  $\nu$  and density  $\rho$ .

The relations in eq 5 and eq 6 reveal that the temperature dependency of the thermal conductivity of a liquid is significantly affected by the coefficient of thermal expansion and the pressure dependency mainly by the compressibility. Assuming in a first assumption  $\gamma_G$  to be constant and  $\nu$  to be independent of temperature, eq 5 and eq 6 predict  $(1/\lambda)(\partial\lambda/\partial T)_p$  to be proportional to  $\alpha_p$  and  $(1/\lambda)(\partial\lambda/\partial p)_T$  to  $\kappa_T$ . McLaughlin and colleagues<sup>25,37</sup> plotted  $(1/\lambda)(\partial\lambda/\partial T)_p$  against  $\alpha_p$  and  $(1/\lambda)(\partial\lambda/\partial p)_T$  against  $\kappa_T$  for various liquids. The used data sets included experimental high-pressure data from Bridgman.<sup>12</sup> The results revealed a nearly linear behavior between  $(1/\lambda)(\partial\lambda/\partial T)_p$  and  $\alpha_p$  as well as  $(1/\lambda)(\partial\lambda/\partial p)_T$  and  $\kappa_T$ . Nevertheless, it has to be noted that neither  $\gamma_G$  nor  $\nu$  fully meet the previously made assumptions.<sup>25,27,37</sup>

Figure 8 illustrates  $(1/\lambda)(\partial\lambda/\partial p)_T$  as a function of  $\kappa_T$  for our data. Except for olive oil, the data points also demonstrate an almost linear relationship with a uniform slope over the whole pressure range studied. This behavior was consistent with results of Kamal and McLaughlin for different organic liquids.<sup>25</sup> A linear extrapolation of the data points to  $\kappa_T \rightarrow 0$  reveals that the straight lines miss the point of origin slightly. Due to manifold influencing variables and the simplified

model approach, it is difficult to find precise reasons for this observation.

The density dependency of the thermal conductivity has often been discussed in the literature<sup>26,27</sup> in connection with the  $g$ -value. The latter can be derived from eqs 3 and 6

$$g = \frac{\rho}{\lambda} \left( \frac{\partial \lambda}{\partial \rho} \right)_T = \left( \frac{\partial \ln \lambda_r}{\partial \ln \rho_r} \right) = \left( \gamma_G + \frac{1}{3} \right) \quad (8)$$

Integration of eq 8 delivers

$$\lambda_r(p, T) = \rho_r(p, T)^g \quad (9)$$

The quantity  $g$  was determined from our data by linear regression. The obtained values are provided as Supporting Information (Table S1). The range of  $g$  is between 2.79 and 3.08 and agrees well with values published by Ross et al.<sup>27</sup> for various organic liquids like heptane, propan-1-ol, propan-2-ol, and toluene. Furthermore, with the exception of olive oil (for  $T > 313.15$  K), the  $g$ -values increase slowly with temperature. This effect was also reported by Forsman et al.<sup>26</sup> for heptane and propan-1-ol. In comparison, castor oil indicates the lowest temperature dependency of  $g$ .

Neglecting this temperature effect, the complete set of data points  $(\partial \ln \lambda_r / \partial \ln \rho_r)$  can be described with good accuracy by a linear regression curve with a slope of  $g = 3.05$ . The application of eq 9 and  $g = 3.05$  leads to deviations between

**Table 6.**  $p\lambda T$  Data for Castor Oil with Standard Deviations in Brackets

$p$	$T$	$\lambda$	$T$	$\lambda$	$T$	$\lambda$	$T$	$\lambda$
MPa	K	$\text{mW}\cdot\text{m}^{-1}\cdot\text{K}^{-1}$	K	$\text{mW}\cdot\text{m}^{-1}\cdot\text{K}^{-1}$	K	$\text{mW}\cdot\text{m}^{-1}\cdot\text{K}^{-1}$	K	$\text{mW}\cdot\text{m}^{-1}\cdot\text{K}^{-1}$
0.1	283.5	179.1 (0.1)	293.3	178.3 (0.4)	314.1	176.5 (0.4)	334.6	174.8 (0.9)
25	283.4	184.7 (0.7)	293.3	184.7 (0.1)	314.1	183.3 (0.3)	334.4	182.3 (0.4)
50	283.4	190.9 (0.1)	293.4	190.2 (0.2)	314.0	189.5 (0.5)	334.6	188.7 (0.4)
100	283.3	200.6 (0.1)	293.4	200.4 (0.1)	313.9	200.1 (0.2)	334.4	200.0 (0.2)
150			293.3	209.7 (0.1)	313.8	209.9 (0.1)	334.5	210.1 (0.1)
200			293.4	218.3 (0.2)	314.0	218.6 (0.2)	334.3	219.0 (0.1)
250					314.4	226.9 (0.2)	334.3	227.8 (0.2)
300					314.0	234.8 (0.1)	334.3	235.7 (0.1)
350							334.7	243.3 (0.1)
400							334.7	250.4 (0.2)

calculated and experimental data of around  $(-0.7$  to  $1.4)$  %. Hence, the knowledge of the pressure–density function allows a good estimation of the thermal conductivity as a function of pressure for the organic liquids mentioned.

Figure 9 illustrates the relationship between  $(1/\lambda)(\partial\lambda/\partial T)_p$  and  $\alpha_p$  for the plant oils. The single sets of data points can be fitted to a linear function. However, the agreement between experimental data and this relation is less clear than  $(1/\lambda)(\partial\lambda/\partial p)_T$  versus  $\kappa_T$  (see also Figure 8 as well as Kamal and McLaughlin<sup>25</sup>). The isobaric thermal expansion coefficients decrease with increasing pressure and the coefficients  $(1/\lambda)(\partial\lambda/\partial T)_p$

change the sign at  $\alpha_p = \alpha_{p,\text{crit}}$  and  $p = p_{\text{crit}}$ . While the progression of data points for olive, safflower, and linseed oil intersect the  $\alpha_p$ -axis at  $\alpha_{p,\text{crit}}$  in the range from  $(5.7$  to  $6.1)\cdot 10^{-4} \text{ K}^{-1}$ , castor oil differs in slopes and  $\alpha_{p,\text{crit}}$  ( $\approx 5\cdot 10^{-4} \text{ K}^{-1}$ ). This can probably be ascribed to the different molecular structures of the oils. The corresponding critical pressures  $p_{\text{crit}}$  vary from  $(61$  to  $126)$  MPa (see Supporting Information (Table S2)). These values are much lower compared to other investigated organic liquids like toluene<sup>31</sup> and propan-2-ol<sup>37</sup> ( $p_{\text{crit}} > 300$  MPa).

McLaughlin and colleagues<sup>25,37</sup> give the following relation, which they obtained by linear regression using various experimental data of different organic liquids including that of Bridgman<sup>12</sup>

$$(1/\lambda)(\partial\lambda/\partial T)_p = -2.75\alpha_p + 1.5\cdot 10^{-3} \quad (10)$$

According to eq 10,  $\alpha_{p,\text{crit}} \approx 5.5\cdot 10^{-4} \text{ K}^{-1}$  results, which corresponds to critical pressures of about 300 MPa.<sup>37</sup> A comparison of our data and this relation is given in Figure 9. The latter shows a certain agreement. However, the slopes and the intersection of the  $x$ -axis differ. One reason for this is that Bridgman's thermal conductivity data<sup>12</sup> are likely to contain larger systematic errors in comparison to newer data.<sup>26,27</sup>

Thermal conductivity measurements by Forsman et al.<sup>26</sup> reveal no sign reversal of  $(1/\lambda)(\partial\lambda/\partial T)_p$  for the linear molecules heptane and propan-1-ol at pressures below 600 MPa but do for the branched propan-2-ol molecules. For the first two liquids, they found at 600 MPa values of  $\alpha_{p,\text{crit}} = 0.3\cdot 10^{-4} \text{ K}^{-1}$  and  $0.35\cdot 10^{-4} \text{ K}^{-1}$ , which are considerably lower in comparison to our data and data published by McLaughlin and colleagues.<sup>25,37</sup> The results of our measurements and data from Nieto de Castro et al.<sup>31</sup> for toluene show a sign reversal of  $(1/\lambda)(\partial\lambda/\partial T)_p$  at  $p_{\text{crit}}$

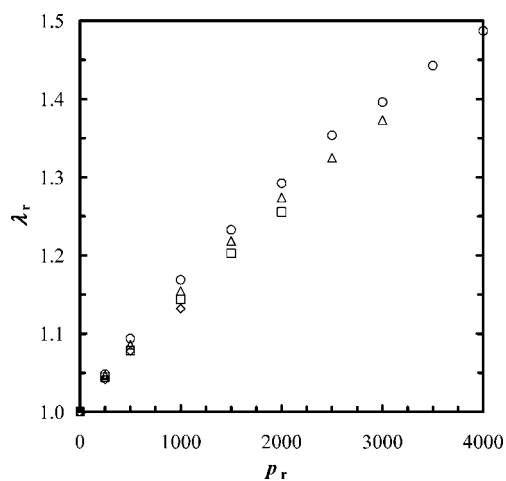


**Figure 3.** Relative thermal conductivity  $\lambda_r = \lambda(p)/\lambda(p_0)$  of olive oil as a function of relative pressure  $p_r = p/p_0$  at different temperatures:  $\diamond$ , 283.2 K;  $\square$ , 293.5 K;  $\triangle$ , 313.9 K;  $\circ$ , 334.4 K.

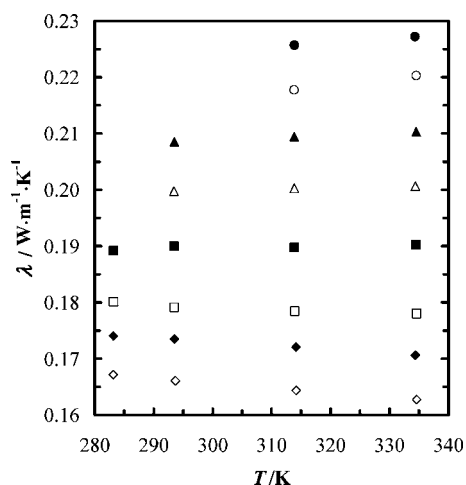


**Figure 4.** Isobars of thermal conductivity  $\lambda$  for olive oil at  $T = (283.1$  to  $334.6)$  K:  $\diamond$ , 0.1 MPa;  $\blacklozenge$ , 25 MPa;  $\square$ , 50 MPa;  $\blacksquare$ , 100 MPa;  $\triangle$ , 150 MPa;  $\blacktriangle$ , 200 MPa;  $\circ$ , 250 MPa;  $\bullet$ , 300 MPa.

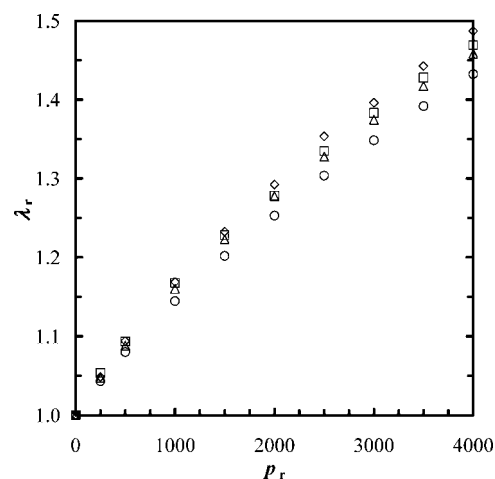


**Figure 5.** Relative thermal conductivity  $\lambda_r = \lambda(p)/\lambda(p_0)$  of plant oils as a function of relative pressure  $p_r = p/p_0$  at  $T = 333$  K:  $\diamond$ , olive;  $\square$ , safflower;  $\triangle$ , linseed;  $\circ$ , castor.

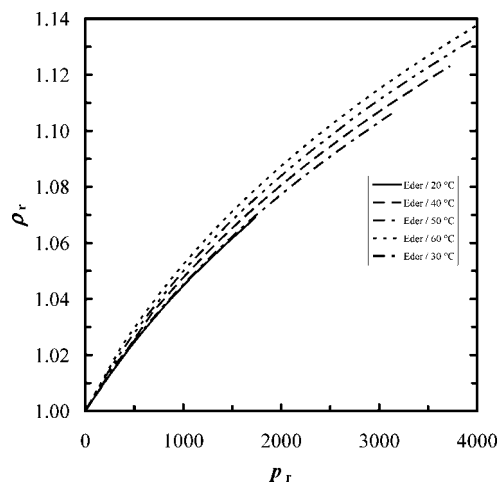


**Figure 6.** Relative density  $\rho_r = \rho(p)/\rho(p_0)$  of olive oil as a function of relative pressure  $p_r = p/p_0$  measured with a Jamin interferometer at different temperatures: —, 293.2 K; -·-·-, 303.2 K; - - -, 313.2 K; -·-·-, 323.2 K; - - - -, 333.3 K.

about 300 MPa. Concerning the differences of the pressure effect on the thermal conductivity of propan-1-ol and propan-2-ol, Forsman et al.<sup>26</sup> supposed that pressure has an ordering effect on the spatial molecule arrangement. This depends on the molecular structure and intermolecular interactions.

Ross et al.<sup>27</sup> provided a simplified explanation for the behavior of the thermal coefficient  $(1/\lambda)(\partial\lambda/\partial T)_p$  discussed above. By combining eqs 5 and 7, one obtains

$$\frac{1}{\lambda} \left( \frac{\partial \lambda}{\partial T} \right)_p = \frac{1}{\lambda} \left( \frac{\partial \lambda}{\partial T} \right)_p - \alpha_p g \quad (11)$$

Previous investigations of different organic liquids revealed that the quantity  $g$  is almost independent of density and not strongly dependent on temperature. Assuming  $(1/\lambda)(\partial\lambda/\partial T)_p$  and  $g$  to be positive and constant, eq 11 shows that simply from thermodynamics it can be expected that  $(1/\lambda)(\partial\lambda/\partial T)_p$  is positive for small  $\alpha_p$  and negative for large  $\alpha_p$ .<sup>27</sup>

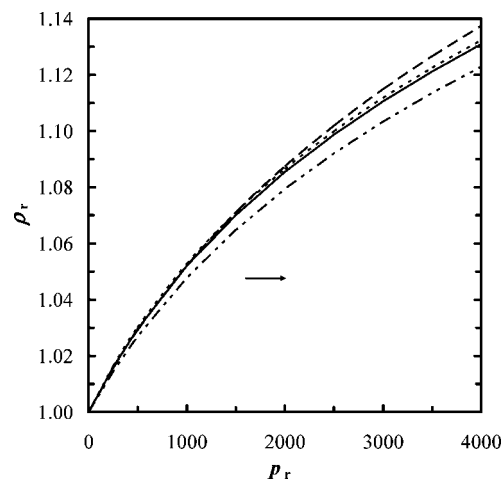


**Figure 7.** Relative density  $\rho_r = \rho(p)/\rho(p_0)$  as a function of relative pressure  $p_r = p/p_0$  for plant oils at  $T = 333$  K: —, olive oil, this work, measured by a Jamin interferometer; - - -, safflower; -·-·-, linseed; ····, castor oil, obtained by the calculation via the Tait equation according to the data of Acosta.<sup>30</sup>

**Molecular Considerations.** The investigated plant oils can be classified according to their fatty acid composition (Table 2). The olive oil is characterized by a high amount of unsaturated oleic acid ( $\approx 75$  %) and about 15 % unsaturated fatty acids. Safflower oil contains mainly linoleic acid ( $\approx 79$  %) and linseed oil linolenic acid ( $\approx 58$  %). Ricinoleic acid ( $\approx 88$  %) can be found only in castor oil. Oleic acid  $C_{18:2(9)}$  is monounsaturated with one double bond in cis-configuration. Due to its inability to rotate at the double bond, the molecule chain tends toward an inflexible bend ( $\approx 40^\circ$ ).<sup>38</sup> Each further cis-double bond in the linoleic acid  $C_{18:2(9,12)}$  and linolenic acid  $C_{18:3(9,12,15)}$  leads to an increased bend of the fatty acid molecule chain.

The shape of the molecule chain influences the geometrical arrangement of the fatty acids to each other within the triglyceride molecule. If bend chains are packed together, the amount of empty space between the chains is naturally reduced in comparison to a straight chain located next to a bent one.<sup>39</sup>

**Table 7. Relative Density  $\rho_r = \rho(p)/\rho(p_0)$  for Olive Oil from Measurements with a Jamin Interferometer from  $T = (293.2$  to  $333.2)$  K and Pressures up to 434 MPa**

T/K = 293.2		T/K = 303.2		T/K = 313.2		T/K = 323.2		T/K = 333.2	
p/MPa	$\rho_r$	p/MPa	$\rho_r$	p/MPa	$\rho_r$	p/MPa	$\rho_r$	p/MPa	$\rho_r$
0.1	1.0000	0.1	1.0000	0.1	1.0000	0.1	1.0000	0.1	1.0000
5.3	1.0028	31.0	1.0168	70.6	1.0361	30.1	1.0175	36.4	1.0228
10.6	1.0056	38.9	1.0202	87.5	1.0234	49.9	1.0277	46.9	1.0280
16.1	1.0085	53.3	1.0265	95.7	1.0265	66.8	1.0357	57.3	1.0332
21.7	1.0113	60.7	1.0297	103.9	1.0297	92.9	1.0469	74.1	1.0411
28.6	1.0145	76.5	1.0328	112.6	1.0328	115.8	1.0559	100.0	1.0523
34.6	1.0174	85.0	1.0361	121.8	1.0361	124.3	1.0591	130.6	1.0642
41.0	1.0204	93.9	1.0394	141.2	1.0428	151.9	1.0688	157.4	1.0737
47.6	1.0234	103.0	1.0428	151.8	1.0462	172.6	1.0756	187.8	1.0837
54.5	1.0265	112.7	1.0462	162.8	1.0497	195.4	1.0826	199.0	1.0871
61.7	1.0296	133.4	1.0568	174.4	1.0532	207.4	1.0862	210.7	1.0907
69.5	1.0328	156.4	1.0643	186.6	1.0568	220.3	1.0899	222.8	1.0942
77.8	1.0362	168.8	1.0681	199.4	1.0605	233.7	1.0937	235.8	1.0979
86.3	1.0395	181.9	1.0721	227.0	1.0681	247.9	1.0976	249.0	1.1016
95.4	1.0430	195.6	1.0761	241.9	1.0721	262.6	1.1015	263.4	1.1055
105.2	1.0465	210.0	1.0801	257.6	1.0761	274.5	1.1048	278.1	1.1094
115.4	1.0502	225.2	1.0843	274.2	1.0801	292.3	1.1092	293.7	1.1134
126.3	1.0539	241.3	1.0886	291.8	1.0843	309.7	1.1134	310.0	1.1174
138.0	1.0578	258.2	1.0929	310.2	1.0886	328.1	1.1177	330.8	1.1224
150.0	1.0616	276.3	1.0974	329.9	1.0929	347.3	1.1221	350.1	1.1268
162.8	1.0656	295.2	1.1020	350.4	1.0974	367.3	1.1265	369.6	1.1312
173.5	1.0691	313.8	1.1064	372.2	1.1020	388.6	1.1311	390.0	1.1356
						410.7	1.1357	411.3	1.1401
						433.8	1.1404	433.6	1.1447

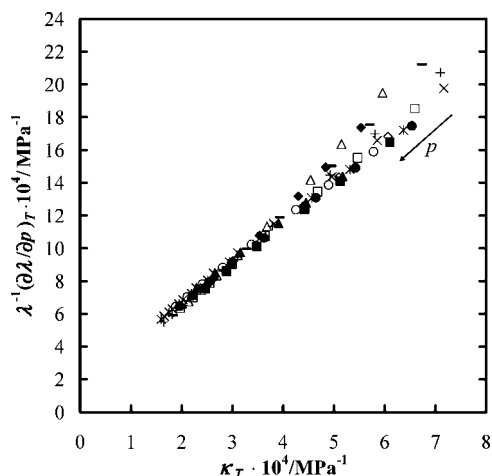


**Figure 8.** Plot of isothermal pressure coefficient of thermal conductivity  $(1/\lambda)(\partial\lambda/\partial p)_T$  versus compressibility  $\kappa_T = (1/\rho)(\partial\rho/\partial p)_T$  for plant oils at different temperatures. Olive:  $\blacklozenge$ , 293 K;  $\triangle$ , 313 K;  $\square$ , 333 K. Safflower:  $\diamond$ , 293 K;  $\square$ , 313 K;  $\times$ , 333 K. Linseed:  $\blacksquare$ , 293 K;  $\bullet$ , 303 K;  $+$ , 333 K. Castor:  $\blacktriangle$ , 293 K;  $\circ$ , 303 K;  $*$ , 333 K. The values of  $(1/\lambda)(\partial\lambda/\partial p)_T$  and  $\kappa_T$  were calculated from our experimentally determined data of thermal conductivity and density results. The high-pressure density data of safflower, linseed, and castor oil were calculated via the Tait equation according to the data of Acosta.<sup>30</sup> The arrow indicates the direction of pressure increase.

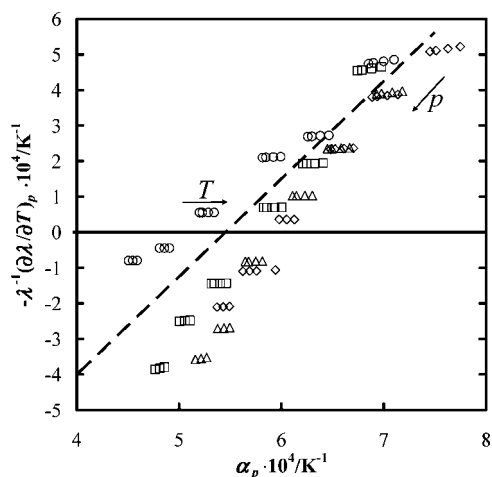


**Figure 9.** Plot of the isobaric thermal coefficient of thermal conductivity  $(1/\lambda)(\partial\lambda/\partial T)_p$  versus thermal expansion coefficient  $\alpha_p = -(1/\rho)(\partial\rho/\partial T)_p$  in the range of  $T = (283 \text{ to } 333) \text{ K}$ :  $\diamond$ , olive;  $\square$ , safflower;  $\triangle$ , linseed;  $\circ$ , castor;  $-$ , eq 10.<sup>37</sup> The values of  $(1/\lambda)(\partial\lambda/\partial T)_p$  and  $\alpha_p$  were calculated from our data of thermal conductivity and density. The high-pressure density data of safflower, linseed, and castor oil were calculated via the Tait equation according to the data of Acosta.<sup>30</sup> The arrows indicate the direction of temperature and pressure increase.

The density of plant oils should therefore increase with content of unsaturated fatty acids. This assumption agrees with the density data for olive, safflower, and linseed oil (Table 2) (see also Nesvadba<sup>22</sup> and Acosta<sup>30</sup>). Castor oil however appears to be an exception due to its high content of the monoacid triglyceride triricinolin ( $\approx 77\%$ ). Furthermore, a polar hydroxyl group exists near one double bond in the ricinoleic acid ( $12\text{-h-C}_{18:1(9)}$ ). In addition to van der Waals forces between the long molecule chains, intermolecular attractive/repulsive forces due to the polar group arise. Hence, these two intermolecular interactions and the monoacid configuration influence the physicochemical properties of this oil. Castor oil has the highest density, thermal conductivity, and viscosity among the plant oils and is in addition characterized by good ethanol solubility.

Apart from castor oil, Acosta et al.<sup>30</sup> describe an analogy between the compressibility of plant oils and its iodine value. The latter is an indicator for the number of double bonds and the amount of unsaturated fatty acids. Their results reveal that the compressibility in general decreases with rising iodine value. Kapranov et al.<sup>33</sup> report that the melting point range of triglycerides increases with pressure. Thus, this phenomenon follows the principle of Le Châtelier. High pressure promotes the formation of denser molecular structures. Concerning the unsaturated fatty acids named above, double bonds in trans-configuration facilitate closer packing because the fatty acid chain is straighter. As a result of this, the melting point increases and is closer to that of triglycerides with saturated chains.<sup>38</sup> Thus, one can assume that high pressures promote a change from the cis- to trans-configuration in the unsaturated fatty acids of triglycerides. This would be connected with a volume reduction and a melting point increase, too.

## Conclusion

The effect of pressure on the thermal conductivity and density of olive, safflower, linseed, and castor oils was investigated up to 400 MPa in the temperature range from (283 to 333) K. The thermal conductivity measurements were carried out by a high-pressure-adapted hot-wire method and the density measurements for olive oil by a high-pressure interferometer.

The most prominent results are: (a) the relative thermal conductivity  $\lambda_r(T,p)$  of the investigated oils increases with pressure; (b) the slopes of the isotherms flatten with rising pressure and decreasing temperature; (c) the increase of  $\lambda_r(T,p)$  decreases in general from olive oil via safflower and linseed oil to castor oil; and (d) the relative density  $\rho_r(T,p)$  data indicate a qualitatively analogous behavior to  $\lambda_r(T,p)$ , but the increase is lower.

Furthermore, investigations concerning the temperature and pressure dependence of the thermal conductivity in association with the vibrational theory<sup>25,27,37</sup> were carried out. The findings show that: (a) the temperature coefficients of the thermal conductivity  $(1/\lambda)(\partial\lambda/\partial T)_p$  of a plant oil depends on its thermal expansion coefficient  $\alpha_p$ ; (b)  $(1/\lambda)(\partial\lambda/\partial T)_p$  is proportional to  $\alpha_p$  in a nearly linear manner; (c)  $\alpha_p$  decreases with increasing pressure, and  $(1/\lambda)(\partial\lambda/\partial T)_p$  changes its sign at  $\alpha_p = \alpha_{p,\text{crit}}$ ; (d)  $\alpha_{p,\text{crit}}$  varies with the type of oil in the range from ( $\approx 5.0$  to  $6.1$ )  $\cdot 10^{-4} \text{ K}^{-1}$  and the corresponding critical pressures between ( $\approx 60$  and  $126$ ) MPa; (e) the pressure coefficients of the thermal conductivity  $(1/\lambda)(\partial\lambda/\partial T)_T$  of a plant oil are a function of its compressibility  $\kappa_T$ ; and (f)  $(1/\lambda)(\partial\lambda/\partial T)_T$  is proportional to  $\kappa_T$  in a nearly linear manner and almost independent of temperature.

The different fatty acid composition of the investigated oils influences their physical properties (e.g., density, compressibility, thermal conductivity) due to the differences in molecular structure and intermolecular interactions. With the exception of castor oil, the density of the investigated liquid plant oils in general increases with increasing iodine value,<sup>22</sup> and the compressibility decreases.<sup>30</sup> Hence, as higher density of a given liquid leads to smaller distances between molecules, the collision probability of the oscillating molecules is enhanced and the intermolecular energy transport (thermal conductivity) is improved. The differences in the molecular structure of castor oil in comparison to the other three oils result (a) in a different relationship between  $(1/\lambda)(\partial\lambda/\partial T)_p$  and  $\alpha_p$  and (b) in a different value for  $g = (\partial \ln \lambda_r / \partial \ln \rho_r)$ . As a mean value for all oils, we obtain  $g = 3.05$ . This agrees well with the literature<sup>27</sup> and enables an estimation of the relative thermal conductivity of



our data as a function of the relative density with an uncertainty of about (−0.7 to +1.4) %.

### Supporting Information Available:

A figure showing the thermal conductivity measurement setup and tables of experimental results concerning quantity  $g$ , critical thermal expansion coefficient  $\alpha_{p,crit}$ , and critical pressure  $p_{crit}$  for the plant oils. This material is available free of charge via the Internet at <http://pubs.acs.org>.

### Literature Cited

- Balny, C.; Masson, P.; Heremans, K. High pressure effects on biological macromolecules: from structural changes to alteration of cellular processes. *Biochim. Biophys. Acta* **2002**, *1595*, 3–10.
- Kulisiewicz, L.; Baars, A.; Delgado, A. Effect of high hydrostatic pressure on structure of gelatine gels. *Bull. Polym. Ac. Technol.* **2007**, *55*, 239–244.
- Kilimann, K. V.; Hartmann, C.; Delgado, A.; Vogel, R. F.; Gänzle, M. G. Combined high pressure and temperature induced lethal and sublethal injury of *Lactococcus lactis* - Application of multivariate statistical analysis. *Int. J. Food Microbiol.* **2006**, *109*, 25–33.
- Rademacher, B.; Hichrichs, J. Effects of high pressure treatment on indigenous enzymes on bovine milk: Reaction kinetics, inactivation and potential application. *Int. Dairy J.* **2006**, *16*, 655–661.
- Bauer, B. A.; Knorr, D. The impact of pressure, temperature and treatment time on starches: pressure-induced starch gelatinisation as pressure time temperature indicator for high hydrostatic pressure processing. *J. Food Eng.* **2005**, *68*, 329–334.
- Pehl, M.; Delgado, A. Experimental investigation on thermofluidynamical processes in pressurized substances. In *Trends in High Pressure Bioscience and Biotechnology*; Hayashi, R., Ed.; Elsevier: Amsterdam, 2002; pp 429–435.
- Delgado, A.; Hartmann, Chr. Pressure Treatment of Food: Instantaneous but not Homogeneous Effect. In *Advances in High Pressure Bioscience and Biotechnology II*; Winter, R., Ed.; Springer: Berlin, Heidelberg, NY, 2003; pp 459–464.
- Hartmann, Chr.; Schuhholz, J. P.; Kitsubun, P.; Chapleau, N.; Le Bail, A.; Delgado, A. Experimental and numerical analysis of the thermofluidynamics in a high-pressure autoclave. *Innovative Food Sci. Emerging Technol.* **2004**, *5*, 399–411.
- Delgado, A.; Baars, A.; Kowalczyk, W.; Benning, R.; Kitsubun, P. Towards system theory based adaptive strategies for high pressure bioprocesses. *High Pressure Res.* **2007**, *27*, 7–16.
- Eder, C.; Delgado, A. Interferometric measurement of the density of aqueous solutions under ultra-high hydrostatic pressure. *Technisches Messen* **2007**, *74*, 45–50.
- Baars, A.; Rauh, C.; Delgado, A. High pressure rheology and the impact on process homogeneity. *High Pressure Res.* **2007**, *27*, 77–83.
- Bridgman, P. W. In *The Physics of High Pressure*, 2nd ed.; G. Bell & Sons: London, 1949.
- Lawson, A. W.; Lowell, R.; Jain, A. L. Thermal Conductivity of Water at High Pressures. *J. Chem. Phys.* **1959**, *30*, 643–647.
- Kestin, J.; Sengers, J. V.; Kamgar-Parsi, B.; Levelt Sengers, J. M. H. Thermophysical Properties of Fluid H<sub>2</sub>O. *J. Phys. Chem. Ref. Data* **1984**, *13*, 175–183.
- Abdulagatov, I. M.; Magomedov, U. B. Thermal conductivity of aqueous solutions of NaCl and KCl at high pressures. *Int. J. Thermophys.* **1994**, *15*, 401–413.
- Denys, S.; Hendrickx, M. E. Measurement of the Thermal Conductivity of Foods at High Pressure. *J. Food Sci.* **1999**, *64*, 709–713.
- Ramaswamy, R.; Balasubramaniam, V. M.; Sastry, S. K. Thermal conductivity of selected liquid foods at elevated pressures up to 700 MPa. *J. Food Eng.* **2007**, *83*, 444–451.
- Kaye, G. W. C.; Higgins, W. F. The thermal conductivity of certain liquids. *Proc. R. Soc. London* **1928**, *A117*, 459–470.
- Nowrey, J. E.; Woodams, E. E. Thermal conductivity of a vegetable oil-in-water emulsion. *J. Chem. Eng. Data* **1968**, *13* (3), 297–300.
- Nesvadba, P. Thermal properties of unfrozen foods. In *Engineering properties of foods*, 3rd ed.; Rao, M. A., Rizvi, S. S. H., Datta, A. K., Eds.; Taylor & Francis: Boca Raton, New York, London, Singapore, 2005; pp 149–173.
- Qashou, M. S.; Vachon, R. I.; Touloukian, Y. S. Thermal conductivity of foods. *ASHRAE Trans.* **1972**, *78*, 165–183.
- Coupland, J. N.; McClements, D. J. Physical properties of liquid edible oils. *JAOCs* **1997**, *74*, 1559–1564.
- Choi, Y.; Okos, M. R. Effects of temperature and composition on the thermal properties of foods. In *Food Engineering and Process Applications - Transport Phenomena*, 1st ed.; Le Ma-guer, M., Jelen, P., Eds.; Elsevier: New York, 1986; pp 93–101.
- Hemminger W. In *Thermophysikalische Stoffgrößen*; Blanke, W., Ed.; Springer: Berlin, 1989; Chapter 5.
- Kamal, I.; McLaughlin, E. Pressure and volume dependence of the thermal conductivity of liquids. *Trans. Faraday Soc.* **1964**, *60*, 809–816.
- Forsman, H.; Andersson, P.; Bäckström, G. Thermal conductivity and heat capacity of n-heptane, n- and iso-propyl-alcohol at high pressure. *Physica* **1982**, *114B*, 287–294.
- Ross, R. G.; Andersson, P.; Sundquist, B.; Bäckström, G. Thermal conductivity of solids and liquids under high pressure. *Rep. Prog. Phys.* **1984**, *47*, 1347–1402.
- Wakeham, W. A. Thermal conductivity of liquids under pressure. *High Temp. High Press.* **1989**, *21*, 249–259.
- Werner, M.; Baars, A.; Werner, F.; Eder, C.; Delgado, A. The thermal conductivity of aqueous sugar solutions under high pressure. *Int. J. Thermophys.* **2007**, *28*, 1161–1180.
- Acosta, G. M.; Smith, R. L.; Arai, K. High-pressure pVT behavior of natural fats and oils, trilaurin, triolein, and n-tridecane from 303 to 353 K from atmospheric pressure to 150 MPa. *J. Chem. Eng. Data* **1996**, *41*, 961–969.
- Nieto de Castro, N. C. A.; Li, S. F. Y.; Maitland, G. C.; Wakeham, W. A. Thermal conductivity of toluene in the temperature range 35–90°C at pressure up to 600 MPa. *Int. J. Thermophys.* **1983**, *4*, 311–327.
- Greger, R.; Delgado, A.; Rath, H. J. *Measurement of the thermal conductivity of fluids with low viscosity under microgravity*. Proceedings of the IUTAM Symposium on Microgravity Fluid Mechanics. 2–6 September 1991; Rath, H. J., Ed.; Springer: Berlin, Heidelberg, 1992; pp 511–515.
- Kapranov, S. V.; Hartmann, C.; Baars, A.; Delgado, A. On the influence of high pressure on edible oils. In *Advances in high pressure bioscience and biotechnology II*; Winter, R., Ed.; Springer: Berlin, 2003; pp 453–457.
- Ramires, M. L. V.; Fareleira, J.M.N.A.; Nieto de Castro, C. A.; Dix, M.; Wakeham, W. A. The thermal conductivity of toluene and water. *Int. J. Thermophys.* **1993**, *14*, 1119–1130.
- Nieto de Castro, C. A.; Li, S. F. Y.; Nagashima, A.; Trengova, R. D.; Wakeham, W. A. Standard reference data for the thermal conductivity of liquids. *J. Phys. Chem. Ref. Data* **1986**, *15*, 1077–1086.
- Horrocks, J. K.; McLaughlin, E. Thermal conductivity of simple molecules in the condensed state. *Trans. Faraday Soc.* **1960**, *56*, 206–212.
- Horrocks, J. K.; McLaughlin, E. Temperature dependence of the thermal conductivity of liquids. *Trans. Faraday Soc.* **1963**, *59*, 1709–1716.
- Belitz, H.-D.; Grosch, W.; Schieberle, P. *Lehrbuch der Lebensmittelchemie*, 5th ed.; Springer: Berlin, New York, London, Paris, 2001.
- Blaurock, A. E. Fundamental understanding of the crystallization of oils and fats. In *Physical properties of fats, oils, and emulsifiers*; Widlak, N., Ed.; AOCS Press: Champaign, IL, 1999; pp 1–2.

Received for review November 20, 2007. Accepted April 1, 2008. This work has been supported financially in part by the Deutsche Forschungsgemeinschaft (German Science Foundation) within the project DFG FOR 358/1-A3, the Bundesministerium für Bildung und Forschung (Federal Ministry of Education and Research) within the project 0330098A, and the Commission of the European Communities, Framework 6, Priority 5 'Food Quality and Safety', Integrated Project NovelQ FP6-CT-2006-015710.

JE700685Q